Available online at www.sciencedirect.com
ScienceDirect
Journal of the European Ceramic Society 27 (2007) 4261–4264
www.elsevier.com/locate/jeurceramsoc

# Effect of Y and Dy co-doping on electrical conductivity of ceria ceramics

S.K. Tadokoro, E.N.S. Muccillo *

*Instituto de Pesquisas Energéticas e Nucleares, CMDMC, R. do Matão, Travessa R, 400, Cidade Universitária, Sao Paulo, SP 05508000, Brazil*

Available online 2 May 2007

**Abstract**

The effect of co-joint additions of Y and Dy on the electrical conductivity of ceria ceramics was studied by impedance spectroscopy. Powder materials were synthesized by aqueous coprecipitation to obtain $Ce_{1-x}(Y_{0.5}Dy_{0.5})_xO_{2-\delta}$ with $0 \leq x \leq 0.15$. Sintering of powder compacts was carried out at 1450 °C for 4 h. The main results show that high densification (~95% of theoretical value) was attained for all compositions. Raman spectroscopy results evidenced the solid solution formation among cerium, yttrium and dysprosium. The electrical conductivity of sintered specimens varies with the total dopant content. A maximum conductivity value was obtained for a lower dopant content considering the behaviour of singly doped ceramics. Moreover, sintered specimens with the same total dopant content exhibit similar electrical conductivity values suggesting that the concentration of oxygen vacancies play a major role in the conduction process of co-doped ceramics.


*Keywords:* Chemical preparation; $CeO_2$; Microstructure-final; Impedance; Fuel cells

## 1. Introduction

Solid electrolytes exhibiting high oxygen-ion conductivity are of special interest for applications in electrochemical devices such as oxygen sensors, oxygen separation membranes and solid oxide fuel cells (SOFCs).[1,2]

Solid solutions of ceria and rare earths have been regarded as promising solid electrolytes for intermediate temperature SOFCs operation because of their high ionic conductivity.[3–6] The major restriction associated to these solid electrolytes is the increase of the electronic conductivity at high temperatures and low oxygen partial pressures as a consequence of $Ce^{4+}$ to $Ce^{3+}$ reduction. One approach to overcome this problem is the use of a co-dopant. In principle, the minoritary dopant should be able to enlarge the electrolytic domain and/or to increase the ionic conductivity of ceria-based solid solutions. Several combinations of additives have been reported in the literature, but most frequently two or more rare earth cations have been focused.[5,7–9]

In this work, solid electrolytes of $Ce_{1-x}(Y_{0.5}Dy_{0.5})_xO_{2-\delta}$ with $0 \leq x \leq 0.15$ were synthesized by the hydroxide coprecipitation to verify the effect of dysprosia co-addition on microstructural and electrical properties of these ceramics. For comparison purposes, the solid solution $Ce_{0.85}Y_{0.15}O_{2-\gamma}$ was also prepared by the same method. Dysprosia was chosen as a co-dopant due to its structural properties, stable valence and suitable cationic radius, along with the relatively high ionic conductivity and high resistance to reduction exhibited by the ceria–dysprosia solid electrolyte.[10]

## 2. Experimental

Cerium nitrate hexahydrate (99.99%, Aldrich), yttrium oxide (99.99%, Sigma Chem. Co) and dysprosium oxide (99%, Merck) were used as starting materials. Solid solutions of $Ce_{1-x}(Y_{0.5}Dy_{0.5})_xO_{2-\delta}$ with $0 \leq x \leq 0.15$ were synthesized by the precipitation of cerium, yttrium and dysprosium hydroxides using ammonium hydroxide as precipitant agent. For comparison purposes, the solid solution $Ce_{0.85}Y_{0.15}O_{2-\gamma}$, hereafter called standard composition, was also prepared by the same method. A full description of experimental procedures may be found elsewhere.[11] Cylindrical pellets were prepared from powders calcined at 400 °C for 2 h, by uniaxial pressing at 98 MPa in a 10 mm diameter stainless steel die. Green compacts were sintered in air for 4 h at 1450 °C.

* Corresponding author. Tel.: +55 11 38169343; fax: +55 11 38169343.
*E-mail addresses:* sktadokoro@click21.com.br (S.K. Tadokoro), enavarro@usp.br (E.N.S. Muccillo).

0955-2219/$ – see front matter © 2007 Elsevier Ltd. All rights reserved.
doi:10.1016/j.jeurceramsoc.2007.02.138

X-ray diffraction experiments were carried out in a diffractometer (D8 Advance, Bruker-AXS) operating at 40 kV and 40 mA using Cu Kα radiation. For crystallite size measurements scans were conducted at 0.01° for 5 s in the $25^\circ \leq 2\theta \leq 31^\circ$ range and the Scherrer equation was used. Raman microscopy (model 3000, Renishaw Raman microscope) was also used for structural characterization. The excitation radiation at 632.8 nm of a He–Ne laser was employed. Representative micrographs were obtained in a scanning electron microscope (XL30, Philips). Average grain size, $G$, values were determined by the intercept method. Impedance spectroscopy measurements were carried out using an impedance analyzer (4192A, Hewlett Packard). Measurements were performed in the 5 Hz to 13 MHz frequency range, and 200–400 °C temperature range. Silver electrodes were used in these measurements. The temperature dependence of the electrical conductivity, $\sigma$, of studied samples was obtained from the usual Arrhenius relation: $\sigma T = \sigma_0 \exp(-E/kT)$, where $\sigma_0$ is the pre-exponential factor, $E$ the apparent activation energy for electrical conduction, $k$ the Boltzmann constant, and $T$ is the absolute temperature.

## 3. Results and discussion

The relative densities of all sintered pellets were 95–97% except for the nominally pure ceria, which was only ≅91%. Average values of crystallite size of sintered pellets estimated by the Scherrer equation are shown in Table 1. It is worth to note that both pure ceria and the standard composition pellet have similar crystallite sizes (∼100 nm). A monotonic decrease of the crystallite size with increasing the total additive content may be observed. It may be inferred from this result that dysprosia is responsible for the reduction in the coherent domain of diffraction in these solid electrolytes. This means that the substitution of Dy for Ce into the $CeO_2$ crystal lattice produces a structural imperfection, due to lattice relaxation, which gives rise to a distribution of intensities around each reciprocal-lattice point. The same effect is not significant when Y substitutes for Ce in the $CeO_2$ lattice.

Raman spectra of some sintered pellets are shown in Fig. 1. These spectra display an intense Raman band with maximum amplitude near 465 $cm^{-1}$, which is characteristic of the triple degenerated $T_{2g}$ mode of the cubic fluorite-type structure. Doped pellets show two other Raman bands (∼520 and ∼650 $cm^{-1}$) attributed to oxygen vacancies created by doping.[12] In effect, the Raman spectrum of pure ceria does not show any band

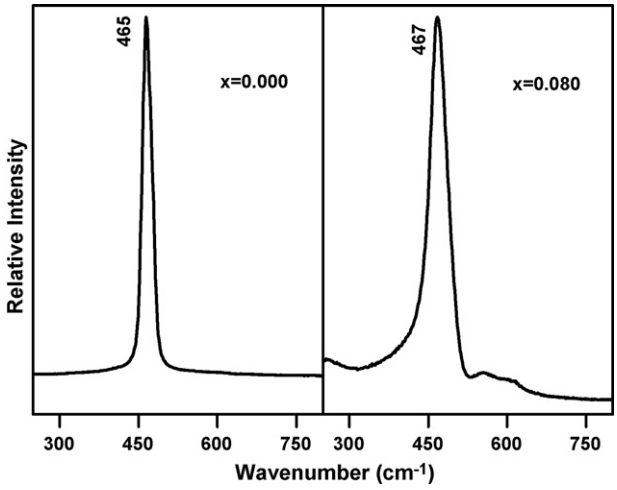


Fig. 1. Raman spectra of pure ceria ($x = 0.0$) and $Ce_{1-x}(Y_{0.5}Dy_{0.5})_xO_{2-\delta}$ ($x = 0.08$).

in this spectral range. It is also important to remark that no Raman band is detected at ∼ 375 $cm^{-1}$, which is typical of the solid solution formed between yttria and dysprosia.[13] This result demonstrates the homogeneous distribution of dopants by this method of synthesis.

Fig. 2 shows SEM micrographs of polished and thermally etched surfaces of sintered pellets with different additive contents. The microstructure of pure ceria (Fig. 2a) is characterized by large grains with closed pores and interconnected pores on grain boundaries and triple junctions. Doped and co-doped pellets, in contrast, show negligible porosity and grains with comparatively smaller size. The average grain size (Table 1) decreases with increasing dopant content up to a steady state value of ∼1.5 μm for $x \geq 0.045$ in $Ce_{1-x}(Y_{0.5}Dy_{0.5})_xO_{2-\delta}$. Considering the standard composition and that with $x = 0.15$, i.e., samples with the same total additive content, it may be concluded that the type of additive has little influence on the final grain size.

Impedance diagrams of sintered pellets are constituted by two well-resolved semicircles attributed to the resistive and capacitive effect of grains (high-frequency semicircle) and blocking of charge carriers at grains boundaries (low-frequency semicircle). The temperature-dependence of the ionic conductivity of studied compositions is shown in Fig. 3. Grain conductivity, $\sigma_g$, values were obtained from the diameter of the high-frequency semicircle and sample dimensions. The grain-boundary conductivity,

Table 1
Values of crystallite size ($t_s$), grain size ($G$), and apparent activation energy for grain ($E_g$) and grain boundary ($E_{gb}$) conductivity

| | $t_s$ (nm) | $G$ (μm) | $E_g$ (eV) | $E_{gb}$ (eV) |
|---|---|---|---|---|
| $x$ in $Ce_{1-x}(Y_{0.5}Dy_{0.5})_xO_{2-\delta}$ | | | | |
| 0.000 | 97.5 ± 0.5 | 16.2 ± 0.7 | 0.82 ± 0.05 | – |
| 0.030 | 83.2 ± 0.5 | 2.4 ± 0.7 | 0.77 ± 0.05 | 1.05 ± 0.05 |
| 0.045 | 62.0 ± 0.5 | 1.6 ± 0.7 | 0.82 ± 0.05 | 0.95 ± 0.05 |
| 0.065 | 49.3 ± 0.5 | 1.5 ± 0.7 | 0.80 ± 0.05 | 0.97 ± 0.05 |
| 0.080 | 51.0 ± 0.5 | 1.6 ± 0.7 | 0.94 ± 0.05 | 0.95 ± 0.05 |
| 0.150 | 34.6 ± 0.5 | 1.4 ± 0.7 | 0.91 ± 0.05 | 0.93 ± 0.05 |
| $Ce_{0.85}Y_{0.15}O_{2-\gamma}$ | 101.1 ± 0.5 | 1.6 ± 0.7 | 0.87 ± 0.05 | 0.93 ± 0.05 |

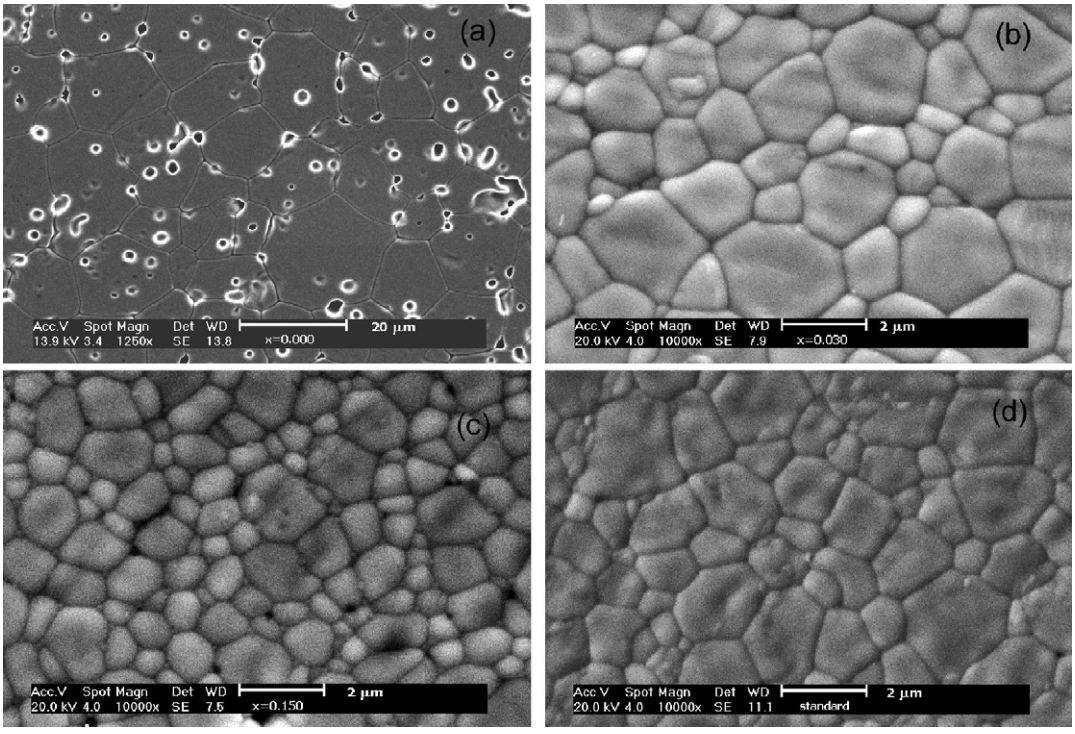


Fig. 2. SEM micrographs of (a) pure ceria, (b) $x = 0.03$, (c) $x = 0.15$ and (d) standard composition sintered pellets.

$\sigma_{gb}$, was calculated from the diameter of the low-frequency semicircle and sample dimension. Temperature-dependent conductivity plots may be fitted by a single straight line in the limited temperature range of measurements. Moreover, the slopes in these plots do not greatly differ, showing a similar mechanism for conduction for all studied compositions. The Arrhenius plots in Fig. 3a shows that almost all sintered pellets containing yttrium oxide and dysprosium oxide as additives, exhibit higher grain conductivity than the standard composition. Apparent activation energy values for grain conductivity, $E_g$, are shown in Table 1. Those pellets with $x = 0.08$, 0.15 and the standard composition have a higher activation energy than other co-doped and pure ceria pellets. This may be a result of association between the dopant cation and the oxygen vacancy. Alternatively, this effect may be related to constraints originated from local cationic arrangements.

The grain boundary conductivity (Fig. 3b) is quite low for pellets with $x = 0.03$, but increases considerably for $x = 0.045$ in $Ce_{1-x}(Y_{0.5}Dy_{0.5})_xO_{2-\delta}$. Values of the apparent activation energy for grain boundary conduction, $E_{gb}$, are shown in Table 1. In this case, the activation energy values are fairly constant ($0.95 \pm 0.02$ eV) for all, except the low-dopant content pellet. The relatively high activation energy of that composition may explain the low grain boundary conductivity shown in Fig. 3b.

The isothermal conductivity of grains and grain boundaries increases up to a given total dopant content and then steadily decreases. The maximum value for the grain conductivity is attained for $x = 0.045$, whereas the grain boundary conductivity is maximum at $x = 0.08$. These results establish a compromise between a maximization of the grain conductivity and minimization of the blocking effect. It should be remarked in Fig. 3, the

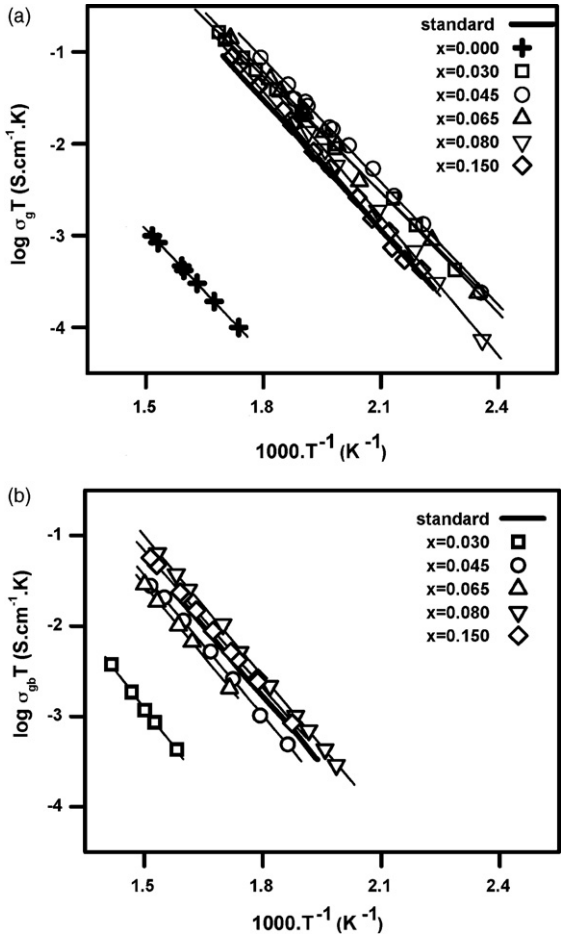


Fig. 3. Temperature dependence of grain (a) and grain boundary (b) conductivity of sintered pellets.

similar conductivity of pellets with the same total dopant content ($x = 0.15$ and that of standard composition). This is evidence that the conduction process in co-doped ceria ceramics is mainly controlled by the oxygen-vacancy concentration.

## 4. Conclusions

Microstructurally homogeneous solid solutions of $Ce_{1-x}(Y_{0.5}Dy_{0.5})_xO_{2-\delta}$ were prepared by the coprecipitation technique. The average grain size of sintered pellets decreases with doping up to $x = 0.045$, and beyond this doping level it is almost constant. The isothermal conductivity of grain and grain boundaries increases for lower co-dopant contents, and after reaching a maximum value, decreases with further increase in the doping level. The grain conductivity of several co-doped pellets was found to be higher than that of yttria-doped ceria. The concentration of oxygen vacancies plays a key role in the electrical conductivity of co-doped pellets.

## Acknowledgements

To FAPESP, CNPq and CNEN for financial support. S.K. Tadokoro acknowledges FAPESP (#00/08908-1) for the scholarship.

## References

1. Goodenough, J. B., Manthiram, A., Paranthaman, M. and Zhen, T. S., Oxide ion electrolytes. *Mater. Sci. Eng. B*, 1992, **12**, 357–364.
2. Minh, N. Q., Ceramic fuel cells. *J. Am. Ceram. Soc.*, 1993, **76**, 563–572.
3. Inaba, H. and Tagawa, H., Ceria-based solid electrolytes—review. *Solid State Ionics*, 1996, **83**, 1–16.
4. Doshi, R., Richards, V. L., Carter, J. D., Wang, X. and Krumpelt, M., Development of solid-oxide fuel cells that operate at 500 °C. *J. Electrochem. Soc.*, 1999, **146**, 1273–1278.
5. Steel, B. C. H., Appraisal of $Ce_{1-y}Gd_yO_{2-y/2}$ electrolytes for IT-SOFC operation at 500 °C. *Solid State Ionics*, 2000, **129**, 95–110.
6. Kharton, V. V., Figueiredo, F. M., Navarro, L., Naumovich, E. N., Kovalevsky, A. V., Yaremchenko, A. A. *et al.*, Ceria-based materials for solid oxide fuel cells. *J. Mater. Sci.*, 2001, **36**, 1105–1117.
7. Herle, J. V., Seneviratne, D. and McEvoy, A. J., Lanthanide co-doping of solid electrolytes: ac conductivity behaviours. *J. Eur. Ceram. Soc.*, 1999, **19**, 837–841.
8. Kim, N., Kim, B.-H. and Lee, D., Effect of co-dopant on properties of gadolinia-doped ceria electrolyte. *J. Power Sources*, 2000, **90**, 139–143.
9. Yoshida, H., Deguchi, H., Miura, K., Horiuchi, M. and Inagaki, T., Investigation of the relationship between the ionic conductivity and the local structures of singly and doubly doped ceria compounds using EXAFS measurements. *Solid State Ionics*, 2001, **140**, 191–199.
10. Yahiro, H., Eguchi, K. and Arai, H., Electrical properties and reducibilities of ceria-rare earth oxide systems and their application to solid oxide fuel cell. *Solid State Ionics*, 1989, **36**, 71–75.
11. Tadokoro, S. K. and Muccillo, E. N. S., Effect of solute dispersion on microstructure and electrical conductivity of $Ce_{0.85}Y_{0.13}Pr_{0.02}O_{2-\delta}$ solid electrolyte. *J. Power Sources*, 2006, **154**, 1–7.
12. McBride, B.-J. R., Hass, K. C., Poindexter, B. D. and Weber, W. H., Raman X-ray studies of $Ce_{1-x}RE_xO_{2-y}$, where RE = La, Pr, Nd, Eu, Gd and Tb. *J. Appl. Phys.*, 1994, **76**, 2435–2441.
13. Panitz, J.-C., Mayor, J.-C., Grob, B. and Durish, W., A Raman spectroscopic study of rare earth mixed oxides. *J. Alloy Compd.*, 2000, **303/304**, 340–344.